1-1-1996

Lamp-pumped laser performance of Nd3+:Sr-5(PO4)(3)F operating both separately and simultaneously at 1.059 and 1.328 mu m

X. X. Zhang
University of Central Florida

M. Bass
University of Central Florida

B. H. T. Chai
University of Central Florida

P. J. Johnson

J. C. Oles

Lamp-pumped laser performance of Nd^{3+}:$Sr_5(PO_4)_3F$ operating both separately and simultaneously at 1.059 and 1.328 μm

Cite as: Journal of Applied Physics **80**, 1280 (1996); https://doi.org/10.1063/1.362926
Submitted: 20 November 1995 . Accepted: 29 April 1996 . Published Online: 17 August 1998

X. X. Zhang, M. Bass, B. H. T. Chai, P. J. Johnson, and J. C. Oles

Lamp-pumped laser performance of Nd^{3+}:$Sr_5(PO_4)_3F$ operating both separately and simultaneously at 1.059 and 1.328 μm

X. X. Zhang,[a] M. Bass, and B. H. T. Chai
CREOL-Center for Research and Education in Optics and Lasers, University of Central Florida, Orlando, Florida 32826

P. J. Johnson and J. C. Oles
Lightning Optical Corporation, Tarpon Springs, Florida 34689

(Received 20 November 1995; accepted for publication 29 April 1996)

Lamp-pumped laser performance of Nd^{3+}-doped strontium fluorapatite, $Sr_5(PO_4)_3F$ or S-FAP, has been characterized and compared with that of Nd^{3+}-doped yttrium aluminum garnet (YAG) at both 1.06 and 1.3 μm. Nd^{3+}:S-FAP was found to exhibit lower thresholds and lower slope efficiencies than Nd^{3+}:YAG. The former is attributed to the higher emission cross section, and the latter to lower Nd^{3+} concentration in S-FAP. The 1.3 μm lasing of Nd^{3+}:S-FAP is of particular interest because of its high emission cross section (2.4×10^{-19} cm^2). Q-switched and dual-wavelength lasing operation were also demonstrated in Nd^{3+}:S-FAP. © *1996 American Institute of Physics.* [S0021-8979(96)04915-8]

I. INTRODUCTION

Apatite crystals were grown and demonstrated as promising laser hosts in the late 60's.[1–3] However, due to their poor thermomechanical properties[4] and inadequate crystal quality, the application of apatite crystals as laser hosts was neglected for many years. The use of diode lasers as pump sources greatly reduces the size of the laser crystal required and the thermal load it must bear. As a result the material strength requirements can be appreciably relaxed. Interest in apatite crystals has been renewed recently[5–13] in the search for more efficient materials for diode laser pumping. Nd^{3+}-doped apatite crystals are of special interest because of the availability of large, high quality crystals.[10,14] Strontium fluorapatite, $Sr_5(PO_4)_3F$ or S-FAP, has been shown[11,13] to be one of the best hosts for Nd^{3+} doping among the apatite crystals as demonstrated by excellent laser-pumped laser performance resulting from superior spectroscopic properties.[11,13,15] Nd^{3+}-doped S-FAP has also been demonstrated[11,13] as an excellent 1.328 μm laser. Initial results have demonstrated promising laser performance[16] for Nd^{3+}-doped S-FAP at both 1.059 and 1.328 μm with pulsed flashlamp pumping. It is of great interest to note that Nd^{3+}-doped S-FAP can potentially provide a 589 nm laser source through the sum-frequency generation of its 1.059 and 1.328 μm lines.

Laser performance of Nd^{3+}:S-FAP is reported in this article with both cw and pulsed lamp pumping. The laser threshold was studied as a function of the output coupling transmission. Information was obtained about the passive losses for both 1.059 and 1.328 μm and the ratio of emission cross sections of these two wavelengths. The resonator parameters for dual-wavelength lasing were calculated based on this information. Simultaneous dual-wavelength lasing at 1.059 and 1.328 μm was demonstrated. Q-switched laser performance was studied with flashlamp pumping. The effects of thermal lensing on laser performance are discussed. Comparisons were made with Nd^{3+}:YAG.

II. SPECTROSCOPY

The room-temperature absorption of Nd^{3+}:S-FAP is given in Fig. 1 in comparison with that of Nd^{3+}:YAG. The features in the absorption spectrum of Nd^{3+}:S-FAP are narrower than those of Nd^{3+}:YAG. However, it is interesting to note that the absorption cross section is in general higher in Nd^{3+}:S-FAP than in Nd^{3+}:YAG. For example, the absorption cross section at ~805 nm is[11] 2.26×10^{-19} cm^2 in Nd^{3+}:S-FAP, whereas it is only $\sim1.5\times10^{-19}$ cm^2 at ~809 nm in Nd^{3+}:YAG. It is important to note that the absorption cross section at ~805 nm in Nd^{3+}:S-FAP is comparable to that of Nd^{3+}:YVO_4 which makes both very attractive for diode laser pumping applications.

The room-temperature π-polarization emission spectrum of Nd^{3+}:S-FAP is given in Fig. 2. For comparison, the emission spectra of Nd^{3+}:YVO_4 and Nd^{3+}:YAG are also given in the same figure. The emission of Nd^{3+}:S-FAP is quite unique in two aspects. First of all, each set of transitions, ${}^4F_{3/2}\rightarrow{}^4I_{11/2}$ or ${}^4F_{3/2}\rightarrow{}^4I_{13/2}$, is dominated by a single emission line. Second, the relative intensity of the 1.3 μm emission to the 1.06 μm emission is quite high compared to Nd^{3+}:YVO_4 or Nd^{3+}:YAG. In fact, the ratio is 0.37, 0.24, and 0.18 for Nd^{3+}:S-FAP, Nd^{3+}:YVO_4, and Nd^{3+}:YAG, respectively. The high ratio is common in Nd^{3+}-doped apatite crystals[13] which makes them very attractive as 1.3 μm lasers.

The emission cross section at 1.059 μm in Nd^{3+}:S-FAP has been estimated[11] to be 5.4×10^{-19} cm^2. The radiative lifetime of Nd^{3+}:S-FAP is approximately 300 μs.[11] As a result, Nd^{3+}:S-FAP has an emission cross-section lifetime product which is about 2.5 and 1.5 times greater than that of Nd^{3+}:YAG and Nd^{3+}:YVO_4, respectively.

The apatite crystals are hexagonal having a $P6_3/m$ space group.[17] The spectroscopic properties of Nd^{3+} ions in apatite crystals have been studied by several authors.[2,3,12,18–21] The apatites can be represented chemically by the general for-

[a]Present address: MELLES GRIOT, 19 Midstate Drive, Suite 200, Auburn, MA 01501.

 0021-8979/96/80(3)/1280/7/$10.00

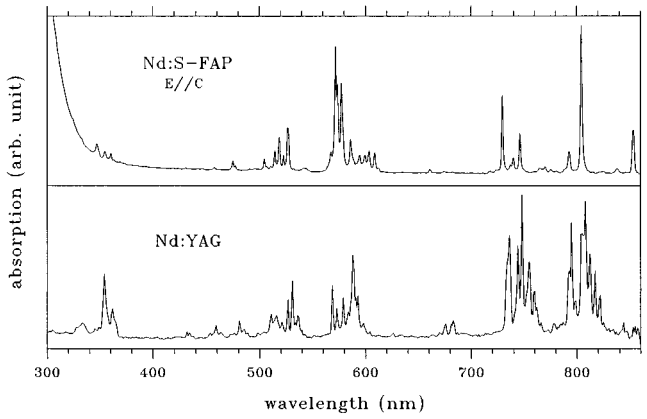

FIG. 1. Room-temperature absorption spectra of Nd^{3+}:S-FAP and Nd^{3+}:YAG (in different arbitrary units).

mula $A_5(MO_4)_3X$, where A is usually an alkaline earth ion, M phosphorus, arsenic, or vanadium, and X a halogen. Nd^{3+} ions substitute at the A sites in apatites. Each unit cell contains two molecules and two crystallographically inequivalent A sites, A_I (40%, ninefold with C_3 symmetry) and A_{II} (60%, sevenfold with C_{1h} symmetry). Despite the fact that there are two inequivalent sites for Nd^{3+} substitution, earlier spectroscopic work[2,19–21] on $Ca_5(PO_4)_3F$, or FAP, suggested that Nd^{3+} ions enter only the A_{II} sites. Our recent high-resolution absorption and site selective spectroscopic studies[12,13,15] indicated that Nd^{3+} ions enter both A_I and A_{II} sites in most of apatites with the exception of S-FAP. This was confirmed by direct measurements using X-ray microprobe experiments.[22]

One of our reasons for developing Nd^{3+}:S-FAP is that there are fewer different substitution sites in S-FAP than in FAP. To illustrate the significance of the multisite substitution, we present in Fig. 3 the emission spectra resulting from the $^4F_{3/2}\rightarrow{}^4I_{11/2}$ transition, excited by a multiline Ar ion laser, for Nd^{3+}:FAP and Nd^{3+}:S-FAP at 15 K. At low temperatures only five lines are expected to result from this transition for a single-site crystal. We can see that the spectrum is much simpler in S-FAP than in FAP.

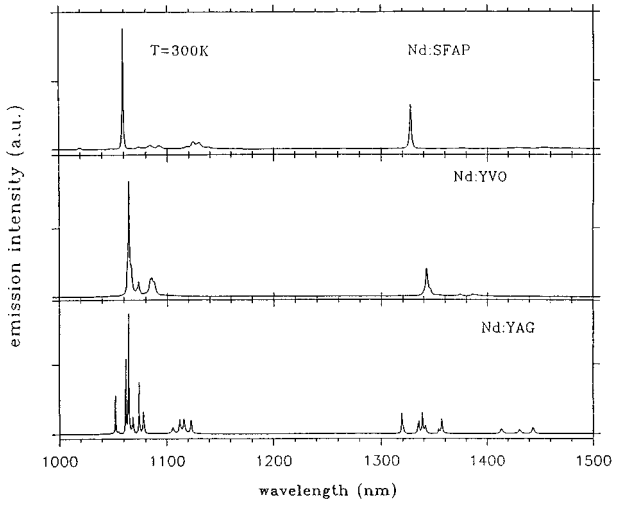

FIG. 2. Room-temperature emission spectra of Nd^{3+} in S-FAP, YVO_4, and YAG (in different arbitrary units).

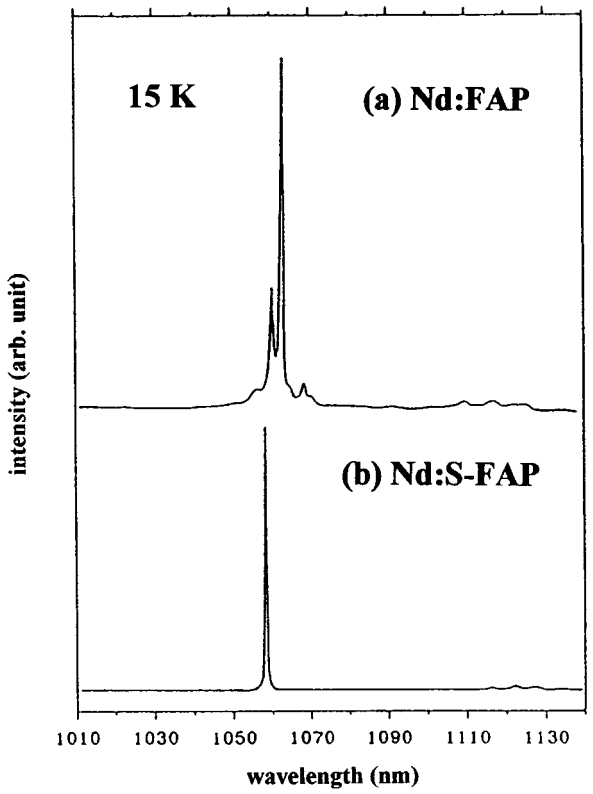

FIG. 3. Low-temperature emission spectra of Nd^{3+} ($^4F_{3/2}\rightarrow{}^4I_{11/2}$) in FAP and S-FAP (in different arbitrary units).

III. LASING PERFORMANCE AT 1.059 AND 1.328 μm SEPARATELY

A. Long-pulsed operation

An S-FAP rod (102 mm in length by 6.3 mm in diameter) containing 1.0 mol % Nd^{3+} in the melt was fabricated for laser testing. Since the distribution coefficient of Nd^{3+} ions in S-FAP is 0.36 (Ref. 3) the actual Nd^{3+} concentration was estimated to be 5.5×10^{19} Nd^{3+} ions/cm^3. The c axis of the crystal was perpendicular to the longitudinal axis of the rod. Both ends of the rod were cut flat and parallel and were antireflection coated at both 1.328 and 1.059 μm with the coating optimized at the former wavelength. The rod was placed inside a 4-in., close-coupled laser head and tested in a Schwartz Electro-Optics Laser 1-2-3 system. A xenon flashlamp was used as the pump source. The distance between the electrodes of the flashlamp was 85 mm and the flashlamp discharge duration was $\sim$300 μs. The optical cavity consisted of a curved high reflector and a flat output coupler about 30 cm apart. The radius of curvature of the high reflector was 50 cm for both wavelengths.

Output couplers with transmission ranging from 10% to 90% for 1.059 μm and from 10% to 48% for 1.328 μm were used in the laser testing. The laser outputs at both wavelengths were linearly polarized along the c axis of the crystal

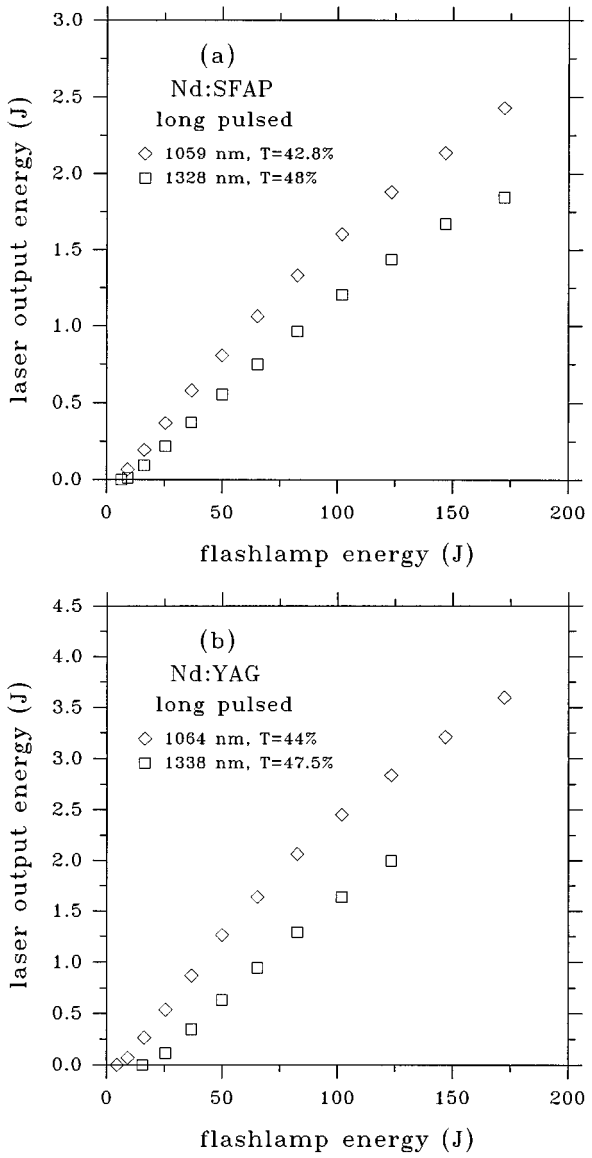

FIG. 4. Typical output energy as a function of input energy of ~1.06 and ~1.3 μm lasers in (a) Nd^{3+}:S-FAP and (b) Nd^{3+}:YAG.

(π polarization). The typical laser output energy as a function of flashlamp energy is given in Fig. 4(a) for both wavelengths. 2.5 J at 1.059 μm and 1.8 J at 1.328 μm can be easily obtained with pump energy of 175 J into the flashlamp. Using a curved output coupler (radius of curvature=50 cm) resulted in an improvement of over 12% in the output energies at high pump levels. The thresholds and slope efficiencies are listed in Table I as a function of the output coupler transmissions for both wavelengths (the slope efficiency was calculated from the linear part of the output-vs-input curve). It can be seen from the table that a slope efficiency of 1.8% for 1.059 μm and 1.3% for 1.328 μm has been achieved and that the slope efficiency does not change much with the output coupling transmission. The thresholds are quite low for both wavelengths.

For comparison an Nd^{3+}:YAG rod (101 mm in length by 6.3 mm in diameter) containing 1.1% Nd^{3+}, or 1.52×10^{20} Nd^{3+} ions/cm^3, was also studied. The rod was cut and polished with flat and parallel end faces. These were antireflection coated at 1.06 μm. The Nd^{3+}:YAG rod was tested in the same laser head using the same cavity as for S-FAP. The laser outputs were not linearly polarized and lasing occurred at 1.064 and 1.338 μm. The typical laser output energy as a function of the flashlamp energy is given in Fig. 4(b). 1.064 μm lasing appeared when attempting 1.338 μm lasing above a certain pump energy. For a 48% output coupler, this pump energy was ~120 J even though both mirrors had >90% transmission at 1.064 μm. The laser thresholds and slope efficiencies of Nd^{3+}:YAG are listed in Table II for the two wavelengths as a function of the output coupling transmission.

Losses in the gain medium can be obtained from the dependence of lasing threshold (E_t) on the output coupler transmission (or reflectivity) using the Findlay–Clay analysis.[23] Assuming 100% reflectivity for the back mirror, this gives

$$E_t = E_0 + (E_0/2\delta L)\ln(R^{-1}), \tag{1}$$

where R is the reflectivity of the output coupler, δ is the total internal loss coefficient, L is the length of the rod, and E_0 is the threshold energy for zero output coupling and can be expressed as

$$E_0 = \delta/A\sigma, \tag{2}$$

where σ is the emission cross section for the laser transition and A is a constant related to the pump efficiency and the quantum efficiency.

The threshold energies are plotted in Fig. 5 as a function of $\ln(R^{-1})$ at both 1.059 and 1.328 μm for Nd^{3+}:S-FAP. One sees that the threshold energy is a linear function of $\ln(R^{-1})$ as Eq. (1) predicts. From the slope and the intercepts we found E_0 and δ, which are listed in Table III. Since the constant A is the same for both 1.059 and 1.328 μm, the ratio of emission cross sections for these two wavelengths can be obtained using Eq. (2) and the E_0 and δ values. This ratio was found to be approximately 2.2 for Nd^{3+}:S-FAP. This ratio is very low compared to other known materials. It is consistent with an earlier estimate based on spectroscopic results and laser-pumped laser performance data.[11] Using the

TABLE I. Laser thresholds and slope efficiencies for various output coupler (O.C.) transmissions for both 1.059 and 1.328 μm in Nd:S-FAP.

Wavelength (μm)	1.059					1.328		
O.C. transmission (%)	10.6	42.8	64.5	71.7	85.5	10.4	34	48
Threshold (J)	1.7	3.3	4.9	5.9	8.6	2.0	4.5	6.4
Slope efficiency (%)	1.5	1.7	1.8	1.8	1.7	1.1	1.3	1.3

TABLE II. Laser thresholds and slope efficiencies for various output coupler (O.C.) transmissions for both 1.064 and 1.338 μm in Nd:YAG.

Wavelength (μm)	1.064					1.338		
O.C. transmission (%)	10.6	44	62	70.5	85.0	10.4	34	47.5
Threshold (J)	2.4	6.3	8.8	9.0	14.5	6.2	13.8	20.3
Slope efficiency (%)	2.1	2.7	2.7	2.7	2.7	1.5	2.0	2.0

emission cross section of 5.4×10^{-19} cm^2 for 1.059 μm in S-FAP,[11] the emission cross section at 1.328 μm should be approximately 2.4×10^{-19} cm^2.

In the same manner as discussed above, results have also been obtained for Nd^{3+}:YAG and are listed in Table III. The emission cross-section ratio of the 1.064 and the 1.338 μm was found to be 3.9. This ratio is consistent with the spectroscopic results. Using the emission cross section of 2.8×10^{-19} cm^2 for Nd^{3+}:YAG,[24] the emission cross section at 1.338 μm was found to be approximately 0.72×10^{-19} cm^2.

Comparing the data in Table I to Table II, we notice that the threshold energies of S-FAP are lower than those of YAG for comparable conditions. The slope efficiencies are, however, ~1.5 times lower in S-FAP than in YAG for both wavelengths The constant A (which is related to the pump efficiency and the quantum efficiency) in Eq. (2) was also found to be a factor of ~1.5 lower in S-FAP than in YAG. Since the quantum efficiency is about the same for both crystals, the difference in A can be attributed to the difference in pump efficiency or absorption efficiency in these two crystals. The slope efficiency is dependent on the pump efficiency and quantum efficiency along with other spectroscopic parameters so that the differences in the slope efficiency between these two crystals can be explained by the difference in A or the difference in absorption efficiency. However, considering that the Nd^{3+} concentration in S-FAP is 2.7 times lower than that of YAG (5.5×10^{19} for S-FAP vs 15×10^{19} ions/cm^3 for YAG), a factor of only 1.5 difference in absorption efficiency indicates that the overall absorption cross section in Nd^{3+}:S-FAP is higher than in Nd^{3+}:YAG. Comparing the absorption spectra in Fig. 1, one realizes that the absorptions are in general narrower in S-FAP than in YAG. This implies that the absorption cross sections of certain individual lines are even higher in S-FAP than in YAG, as mentioned in Sec. II. Therefore better performance for Nd^{3+}:S-FAP can be expected from more concentration-optimized crystals.

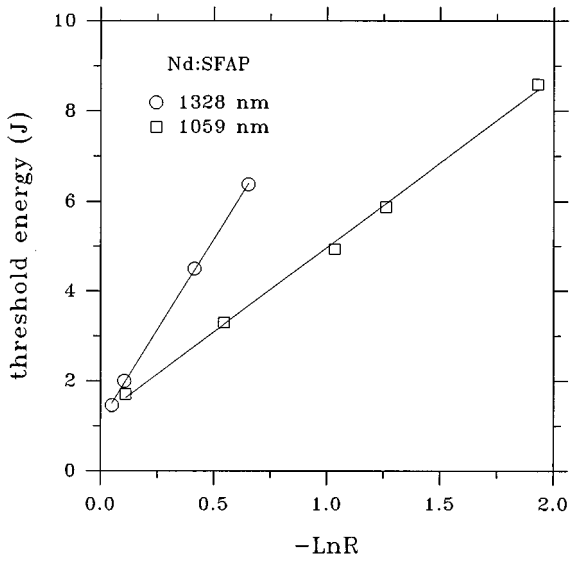

FIG. 5. The laser threshold energy as a function of output coupler reflectivity for 1.059 and 1.328 μm Nd^{3+}:S-FAP lasers.

We notice that the losses at ~1.3 μm are a factor of ~2.5 and ~2 lower than that at ~1.06 μm in S-FAP and YAG, respectively. The relatively high emission cross section and low loss at 1.328 μm makes it very easy to operate Nd^{3+}:S-FAP at this wavelength. In fact, the Nd^{3+}:S-FAP lases at 1.328 μm using a 48% output coupler even when the back mirror has a high reflectivity coating for both 1.328 and 1.059 μm. With this resonator and Nd^{3+}:YAG, only 1.064 μm lasing was detected.

B. *Q*-switched operation

Q-switched operation at both wavelengths was also tested. A KD*P Pockels cell and a Glan prism linear polarizer combination served as the *Q*-switch. The Pockels cell was enclosed in a cell filled with index-matching fluid. The windows were antireflection coated only at 1.06 μm. The polarizer was not coated for either wavelength. The length of the resonator in this case was ~46 cm. High reflectors with a radius of curvature of 50 and 100 cm were used for 1.059 and 1.328 μm, respectively. The results shown in Fig. 6 for Nd^{3+}:S-FAP were obtained with an output coupler having a transmission of 94% for 1.059 μm and 48% for 1.328 μm, respectively. It can be seen that 150 mJ at 1.059 μm and 100 mJ at 1.328 μm have been obtained from Nd^{3+}:S-FAP with pump energies of 35 and 48 J, respectively. The pulse widths were 16 ns for 1.059 μm and 20 ns for 1.328 μm.

Q-switched results for Nd^{3+}:YAG at 1.064 μm are also shown in Fig. 6 for comparison. The highest energy obtained was about the same for both crystals at ~1.06 μm. However,

TABLE III. Comparisons of zero-output-coupling thresholds, passive losses, and emission cross-section ratios for Nd^{3+}:S-FAP and Nd^{3+}:YAG.

Crystal	S-FAP		YAG	
wavelength	1.059 μm	1.328 μm	1.064 μm	1.338 μm
E_0 (J)	1.2	1.1	1.6	3.2
δ (cm^{-1})	0.0165	0.0067	0.0169	0.0084
$\sigma_{1.06\ \mu m}/\sigma_{1.3\ \mu m}$	2.2		3.9	

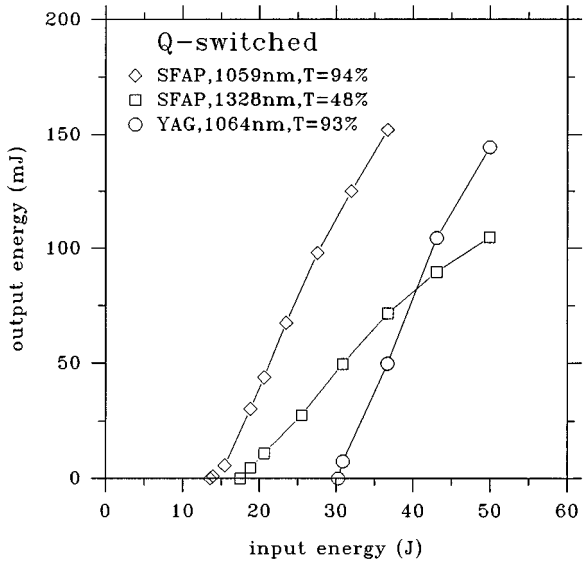

FIG. 6. Q-switched output energy as a function of input energy for Nd^{3+}:S-FAP at 1.059 and 1.328 μm and Nd^{3+}:YAG at 1.064 μm.

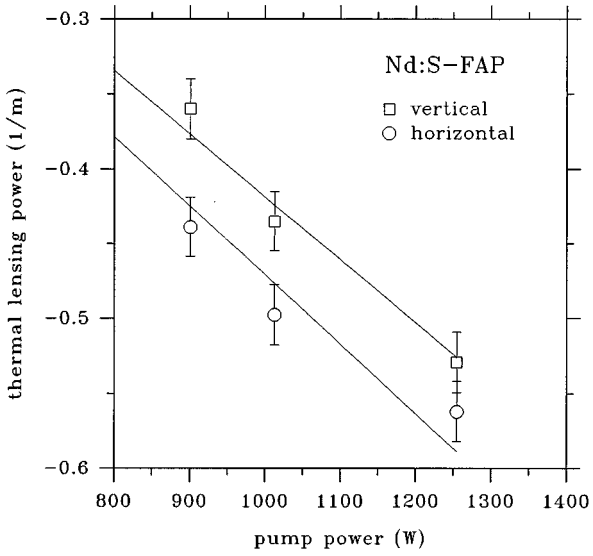

FIG. 7. Thermal lensing power (1/focal length) as a function of pump power in Nd^{3+}:S-FAP.

the threshold for YAG was substantially higher for similar cavities tested. The Q-switched pulse width was slightly longer for YAG than for S-FAP.

In preparing for the 1.3 μm Q-switched operation of Nd^{3+}:YAG, we noticed that 1.319 μm appeared in addition to the 1.338 μm line when either the Pockels cell or the polarizer was present inside the cavity and the pump energy reached about 36 J in long-pulse operation. At this pump level, the Q-switched output was about 40 mJ and irregular temporal pulse shapes were observed. Several pulses were observed under higher pump levels and the output energy was very unstable. Three wavelengths were observed in the red after the output was passed through a nonlinear crystal indicating that the 1.319 and 1.338 μm lines did lase simultaneously though the output was very unstable.

C. cw operation

An S-FAP rod (102 mm in length by 5 mm in diameter) was used in the cw laser testing. The rod was cut from the same boule as the above mentioned one. It was cut and polished with flat and parallel end faces. Both ends were AR coated at both 1.059 and 1.328 μm with the optimization at the latter wavelength. A close-coupled laser head with a Kr lamp (arc length=85 mm) was used. The laser head reflector was gold coated. The laser head was designed for Laser Photonics 100 W Nd^{3+}:YAG lasers. The cooling was provided by deionized flowing water with a flow rate of 2 gal/min. The resonator consisted of a high reflector with a radius of curvature of 50 cm and a flat output coupler. The length of the cavity was 30 cm.

Lasing was achieved at both wavelengths. The laser output was linearly polarized. For 1.059 μm, the threshold was 938 and 987 W for 3.5% and 5% output coupler transmission, respectively. For 1.328 μm, the threshold was 620 ± 50 W (this threshold was too low to be measured directly and so was estimated by extrapolating the input/output curve) for the 3% T output coupler and 692 W for 4.2% T. However, the maximum output obtained was only 1 W for 1.059 and 2.5 W for 1.328 μm with a pump level of $\sim$1.3 kW, above which the output power drops drastically to zero.

We noticed that the threshold was lower and the slope efficiency was higher for the 1.328 than the 1.059 μm. This is probably due to the lower losses at the former wavelength as mentioned in Sec. II A. The drop of the output power for pump powers greater than 1.3 kW is probably due to thermal lensing. We measured the thermal gradient induced focal length of the rod as a function of pump power. The focal length was determined, using simple geometric relations, by measuring the spot sizes of a He-Ne laser beam at a fixed distance after passing the pumped and unpumped rod. It was found that the thermal lensing is negative in Nd^{3+}:S-FAP. That is, the thermal focal length has a minus sign. The measured focal lengths are plotted in Fig. 7 as a function of pump power. It can be seen from the figure that the thermal focal length is of the order of -180 cm when the pump power reaches 1.3 kW. It is interesting to note that the thermal focal power is slightly different in different orientation. The c axis of the rod was vertical and the lamp was horizontally next to the rod in the measurement. ''Vertical'' in the Fig. 7 therefore means the orientation that is parallel to the c axis. The figure indicates that the focal power is lower along the c axis (i.e., the He-Ne laser beam diverges less in the c-axis direction).

IV. DUAL-WAVELENGTH LASING PERFORMANCE

As shown in Sec. II A, the emission cross section at 1.328 μm is quite high in Nd^{3+}:S-FAP. In addition, the loss at this wavelength is much smaller than at 1.06 μm. These are very favorable factors for the realization of simultaneous lasing at both wavelengths.[25] We have measured the laser

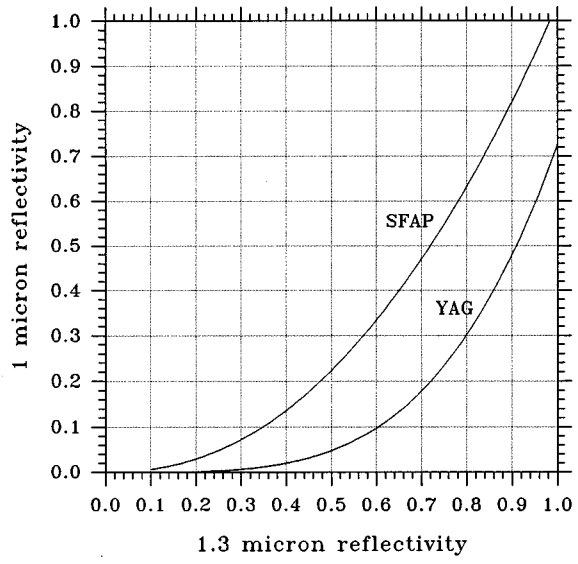

FIG. 8. Design curves for an output coupler enabling dual-wavelength lasing in Nd^{3+}:S-FAP and Nd^{3+}:YAG.

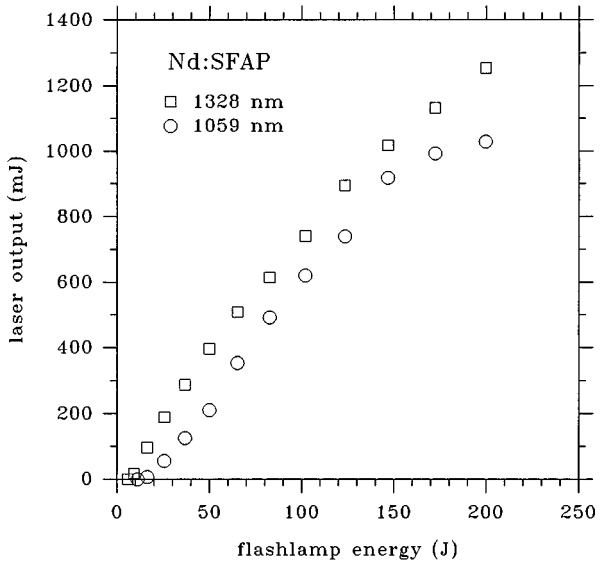

FIG. 9. The laser output energies at each wavelength as a function of input energy for Nd^{3+}:S-FAP when operating simultaneously at 1.059 and 1.328 μm.

threshold as a function of the output coupling transmission. Assuming the condition for simultaneous lasing is that the laser thresholds are the same for both wavelengths:[25]

$$E_{\text{th}}(1.06\ \mu\text{m}) = E_{\text{th}}(1.3\ \mu\text{m}), \tag{3}$$

and according to Eq. (1), we have the following relationships for Nd^{3+}:S-FAP:

$$E_{\text{th}}(1.06\ \mu\text{m}) = 1.23 - 3.66 \ln R_{1.06\ \mu\text{m}}, \tag{4}$$

and

$$E_{\text{th}}(1.3\ \mu\text{m}) = 1.1 - 8.1 \ln R_{1.3\ \mu\text{m}}. \tag{5}$$

Substituting Eqs. (4) and (5) into Eq. (3) we obtain the following:

$$R_{1.06\ \mu\text{m}} = \exp(0.0355 + 2.213 \ln R_{1.3\ \mu\text{m}}). \tag{6}$$

Assuming the back mirror has high reflectivity for both 1.06 and 1.3 μm, the reflectivity at 1.06 μm is determined by Eq. (6) according to the chosen reflectivity at 1.3 μm in order to achieve simultaneous lasing at both wavelengths. Similarly, we obtain the condition for Nd^{3+}:YAG:

$$R_{1.06\ \mu\text{m}} = \exp(-0.321 + 3.928 \ln R_{1.3\ \mu\text{m}}). \tag{7}$$

Plots of Eqs. (6) and (7) are given in Fig. 8. We can see from the figure that there is a wide range of reflectivities for Nd^{3+}:S-FAP to lase simultaneously. We had two mirror coatings prepared at Lightning Optical Corp. to test our predictions. One of them has $R_{1.06\ \mu\text{m}}=31.6\%$ and $R_{1.3\ \mu\text{m}}=54.5\%$, and the other has $R_{1.06\ \mu\text{m}}=35.5\%$ and $R_{1.3\ \mu\text{m}}=55\%$. Simultaneous lasing was achieved for the first coating and not for the second one. This is in good agreement with our predictions. The output energies at each wavelength as a function of pump energy are given in Fig. 9 when simultaneous lasing occurred using the first mirror. It can be seen that more than 1 J has been achieved for each wavelength. The temporal waveforms for each lasing wavelength as well as the waveform of the flashlamp pulse are given in Fig. 10. The simultaneity of both lasing wavelength is indicated in the figure. This was further confirmed by the observation of 589 nm laser emission when a sum-frequency nonlinear crystal was placed in the dual-wavelength output beam path.

V. SUMMARIES AND CONCLUSIONS

In summary, we have characterized and compared the laser performance of Nd^{3+}:S-FAP to that of Nd^{3+}:YAG in lamp-pumped operation. Long-pulse, Q-switched, and cw lasing have been studied. The thresholds were found to be lower in S-FAP thanks to the higher product of radiative lifetime and emission cross section. 2.5 J at 1.059 μm and

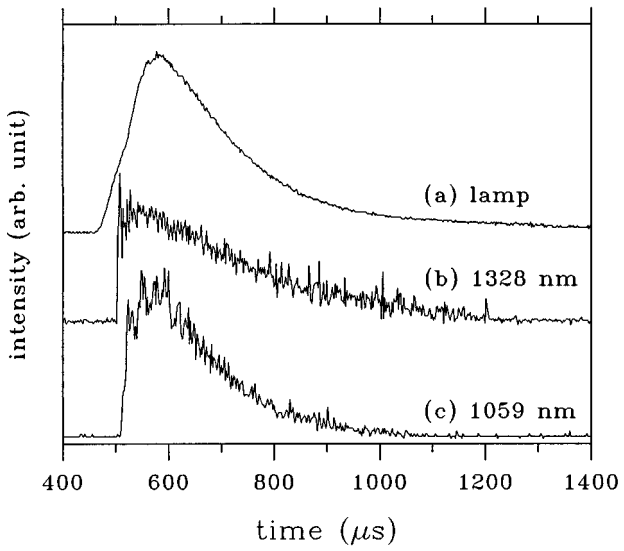

FIG. 10. The lasing temporal waveforms of Nd^{3+}:S-FAP in long-pulse dual-wavelength operation.

1.8 J at 1.328 μm were easily achieved in long-pulse operation using a nonoptimized resonator and a nonoptimized crystal. The pump efficiency was found only a factor of 1.5 lower in S-FAP than in YAG although the Nd^{3+} ion density was a factor of 2.7 lower and the absorption spectrum features are narrower in S-FAP. These results indicate that better laser performance can be expected for S-FAP crystals with higher Nd^{3+} concentrations. It is of interest to note that it has been demonstrated[14] that S-FAP crystals can be grown with an Nd^{3+} concentration five times of that studied in this article.

Our studies indicate that the emission cross section for the $\sim$1.3 μm transition is only a factor of 2.2 lower than that at $\sim$1.06 μm in S-FAP compared to 3.9 in YAG. Consequently, the emission cross section at $\sim$1.3 μm is estimated to be about 3.3 times higher in S-FAP than in YAG (2.4×10^{-19} vs 0.72×10^{-19} cm^2). In addition, the losses were found to be very low at 1.3 μm in S-FAP. These properties make Nd^{3+}:S-FAP particularly attractive as a 1.3 μm laser source. It should find use in a variety of applications that require 1.3 μm lasers. The high emission cross section and low losses also make simultaneous dual-wavelength lasing easy to achieve. In fact, dual-wavelength lasing at 1.059 and 1.328 μm has been successfully demonstrated in the long-pulse mode of operation for Nd^{3+}:S-FAP producing more than 1 J in each wavelength. Spectroscopic data, loss measurements and the preliminary cw testing results indicate that cw dual-wavelength operation should be possible.

Our results indicate that Nd^{3+}:S-FAP develops as a negative thermal lens when a radially symmetric thermal gradient is established in the ac plan of the crystal. This should be taken into account for optimized operation. We are currently investigating this issue in detail.

ACKNOWLEDGMENTS

The authors would like to thank Dr. P. Hong for the spectroscopic work and useful discussions. The technical assistance in the cw experiments provided by Dr. W. Williams and Mr. M. Nunn of Laser Photonics, Inc. is greatly appreciated. This work was supported by the U.S. Department of the Air Force, Wright Laboratory, Eglin AFB, P.O. No. F08630-95-M-0066.

[1] R. Mazelsky, R. H. Hopkins, and W. E. Kramer, J. Cryst. Growth **3/4**, 260 (1968).
[2] R. C. Ohlman, K. B. Steinbruegge, and R. Mazelsky, Appl. Opt. **7**, 905 (1968).
[3] K. B. Steinbruegge, T. Henningsen, R. H. Hopkins, R. Mazelsky, N. T. Melamed, E. P. Riedel, and G. W. Roland, Appl. Opt. **11**, 999 (1972).
[4] R. H. Hopkins, D. H. Damon, P. Piotrowski, M. S. Walker, and J. H. Uphoff, J. Appl. Phys. **42**, 272 (1971).
[5] Z. Shao, Y. Chen, and J. C. Bergquist, Chin. Phys. **11**, 391 (1991).
[6] L. D. Deloach, S. A. Payne, L. L. Chase, L. K. Smith, W. L. Kway, and W. F. Krupke, IEEE J. Quantum Electron. **QE-29**, 1179 (1993).
[7] S. A. Payne, L. K. Smith, L. D. Deloach, W. L. Kway, J. B. Tassano, and W. F. Krupke, IEEE J. Quantum Electron. **QE-30**, 170 (1994).
[8] S. A. Payne, B. H. T. Chai, W. L. Way, L. D. DeLoach, L. K. Smith, G. Lutts, R. Peale, X. X. Zhang, G. D. Wilke, and W. F. Krupke, Conference on Lasers and Electron-Optics (CLEO), Baltimore, 1993, postdeadline paper CPD12.
[9] L. D. Deloach, S. A. Payne, L. K. Smith, W. L. Kway, and W. F. Krupke, J. Opt. Soc. Am. B **11**, 269 (1994).
[10] X. X. Zhang, G. B. Loutts, M. Bass, and B. H. T. Chai, Appl. Phys. Lett. **64**, 10 (1994).
[11] X. X. Zhang, P. Hong, G. B. Loutts, J. Lefaucheur, M. Bass, and B. H. T. Chai, Appl. Phys. Lett. **64**, 3205 (1994).
[12] P. Hong, X. X. Zhang, R. E. Peale, H. Weidner, M. Bass, and B. H. T. Chai, J. Appl. Phys. **77**, 294 (1995).
[13] P. Hong, X. X. Zhang, M. Bass, and B. H. T. Chai, in *Conference on Lasers and Electro-Optics*, Vol. 8, 1994 OSA Technical Digest Series (Optical Society of America, Washington, D.C., 1994), p. 159.
[14] G. B. Loutts and B. H. T. Chai, SPIE Proc. **1863**, 31 (1993).
[15] B. H. T. Chai, G. Loutts, J. Lefaucheur, X. X. Zhang, P. Hong, M. Bass, I. A. Shcherbakov, and A. I. Zagumennyi, in *OSA Proceedings on Advanced Solid-State Lasers*, edited by T. Y. Fan and B. H. T. Chai (Optical Society of America, Washington, DC, 1994), Vol. 20, p. 41.
[16] X. X. Zhang, M. Bass, and B. H. T. Chai, *OSA Proceedings on Advanced Solid-State Lasers*, edited by B. H. T. Chai and S. A. Payne (Optical Society of America, Washington, DC, 1995), Vol. 24, p. 150.
[17] S. Naray-Szabo, Z. Kristallogr. **75**, 387 (1930).
[18] A. M. Morozov, L. G. Morozova, A. K. Trefimov, and P. P. Feofilov, Opt. Spectrosc. **29**, 560 (1970).
[19] C. V. Maksimova and A. A. Sobol, in Proceedings (Trudy) of the P.N. Lebedev Physics Institute, edited by D. V. Skobel'tsyn, Vol. 60, p. 59.
[20] A. A. Kaplyanskii and E. G. Kuzminov, Opt. Spectrosc. **29**, 376 (1970).
[21] F. M. Ryan, R. W. Warren, R. H. Hopkins, and J. Murphy, J. Electrochem. Soc. **125**, 1493 (1978).
[22] D. Corker (personal communications).
[23] D. Findlay and R. A. Clay, Phys. Lett. **20**, 277 (1966).
[24] W. Koechner, *Solid-State Laser Engineering*, 3rd ed. (Springer, Berlin, 1992), p. 49.
[25] H. Y. Shen, R. R. Zeng, Y. P. Zhou, G. F. Yu, C. H. Huang, Z. D. Zeng, W. J. Zhang, and Q. J. Ye, IEEE J. Quantum Electron. **QE-27**, 2315 (1991).